

TOPICAL REVIEW • OPEN ACCESS

## Research prospects of graphene-based catalyst for seawater electrolysis

To cite this article: Xinyu Li *et al* 2023 *Mater. Futures* **2** 042104

View the [article online](#) for updates and enhancements.

You may also like

- [Deposition of VO<sub>x</sub> Films by Reactive Sputtering and its Properties](#)  
Xiaoying Wei, Kailiang Zhang, Wang Fang et al.
- [Effect of pH on CMP of VO<sub>x</sub> Thin Films for RRAM](#)  
Yin Liguo, Kailiang Zhang, Wang Fang et al.
- [Effects of Oxygen Flow Ratios and Annealing on TiO<sub>x</sub> Deposited by Reactive Magnetron Sputtering](#)  
Lanlan Wang, Kailiang Zhang, Qi Wang et al.

## Topical Review

# Research prospects of graphene-based catalyst for seawater electrolysis

Xinyu Li<sup>1</sup>, Yingjie Liu<sup>1</sup>, Yanhui Feng<sup>1</sup>, Yunwei Tong<sup>1</sup>, Zhenbo Qin<sup>1</sup>, Zhong Wu<sup>1,2,\*</sup> , Yida Deng<sup>3,\*</sup> and Wenbin Hu<sup>1,2,4</sup>

<sup>1</sup> Key Laboratory of Advanced Ceramics and Machining Technology of Ministry of Education Tianjin University, Tianjin 300072, People's Republic of China

<sup>2</sup> Key Laboratory of Composite and Functional Materials School of Material Science and Engineering, Tianjin University, Tianjin 300072, People's Republic of China

<sup>3</sup> State Key Laboratory of Marine Resource Utilization in South China Sea, School of Materials Science and Engineering, Hainan University, Haikou 570228, People's Republic of China

<sup>4</sup> Joint School of National University of Singapore and Tianjin University International Campus of Tianjin University, Binhai New City, Fuzhou 350207, People's Republic of China

E-mail: [zhong.wu@tju.edu.cn](mailto:zhong.wu@tju.edu.cn) and [yida.deng@tju.edu.cn](mailto:yida.deng@tju.edu.cn)

Received 27 June 2023, revised 7 August 2023

Accepted for publication 17 August 2023

Published 19 September 2023



CrossMark

## Abstract

Seawater has obvious resource reserve advantages compared to fresh water, and so the huge potential advantages for large-scale electrolysis of hydrogen production has been paid more attention to; but at the same time, electrolysis of seawater requires more stable and active catalysts to deal with seawater corrosion problems. Graphene-based materials are very suitable as composite supports for catalysts due to their high electrical conductivity, specific surface area, and porosity. Therefore, the review introduces the problems faced by seawater electrolysis for hydrogen production and the various catalysts performance. Among them, the advantages of catalysis of graphene-based catalysts and the methods of enhancement the catalytic performance of graphene are emphasized. Finally, the development direction of composite catalysts is prospected, hoping to provide guidance for the preparation of more efficient electrocatalysts for seawater electrolysis.

Keywords: graphene, seawater electrolysis, catalyst

## 1. Introduction

Hydrogen energy is considered to be the ideal and potential energy carrier in the future due to its high efficiency,

pollution-free and simple production. At present, the main means of obtaining hydrogen energy are hydrogen production from fossil fuels [1–3], biological hydrogen production [4–6], solar hydrogen production [7, 8], hydrogen production from electrolysis of water [9–13], etc, among which hydrogen production by electrolysis of water is the most practical method. In industry, the main source of electrolyzed water is fresh water, whereas fresh water resources are extremely scarce and electrolysis of water will exacerbate the shortage of fresh water [14], however, the cost of producing fresh water for electrolysis through desalination of seawater is also extremely high

\* Authors to whom any correspondence should be addressed.



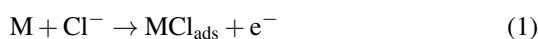
Original content from this work may be used under the terms of the [Creative Commons Attribution 4.0 licence](https://creativecommons.org/licenses/by/4.0/). Any further distribution of this work must maintain attribution to the author(s) and the title of the work, journal citation and DOI.

[15]; Specifically the complex process and high cost equipment are the basic status of seawater desalination, and the seawater desalination process consumes a lot of energy [16–19]. According to a dataset from the Carlsbad Desalination Plant (537 M USD), in San Diego County, USA, Wittholz *et al* [20] investigated the cost of water desalination, and analyzed the breakdowns of the cost, including fixed cost (capital cost) and operating cost (maintenance, material and energy cost, etc), the fixed cost contribute reaches 40% of total costs, while energy costs account for a higher proportion [19]. In seawater desalination, the energy consumption is significant, the primary desalination cost of electrical energy of reverse osmosis (RO) technology is  $2 \sim 4 \text{ kWh m}^{-3}$  [17–19], and the energy consumption accounts for more than 87% of the operating cost [19]. Similarly, Xiang and Liu collected the total cost of representative seawater desalination projects from some literatures and estimated the cost of China's seawater desalination project [21], they found out the energy consumption cost (including electricity cost and heat cost), accounts for 30%–45% of the total cost. Among them, RO industry cost in the range 33%–39% and MED industry for 43%–45%. Therefore, the future research direction of electrolyzed water uses seawater as electrolyte for electrolysis, which can effectively utilize about 96.5% of the earth's water resources and reduce cost, while avoiding problems caused by the scarcity of various freshwater resources [22].

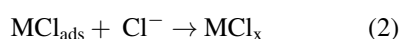
## 2. Electrochemical catalysis mechanism of seawater

Although electrolysis of seawater has broad application prospects, however, many new challenges still need to be faced for electrolyzed seawater compared to fresh water such as seawater corrosion, anode competition, and cathodic deposition issues. Seawater contains a lot of sodium chloride, the presence of  $\text{Cl}^-$  in the electrolyte will corrode the electrode substrate materials and adsorb on the metal catalyst surface, and causing hydroxides on them, thereby blocking the active sites on the electrode and reducing the catalytic performance of the catalyst material for electrolysis of seawater. Its formation mechanism is divided into three processes equations (1)–(3) [2]:

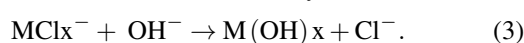
Adsorption of  $\text{Cl}^-$  by surface polarization:



Dissolution by further coordination:



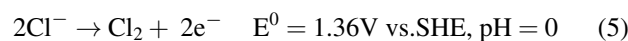
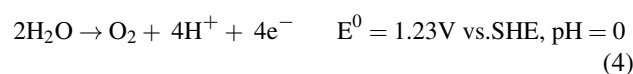
Conversion from chloride to hydroxide:



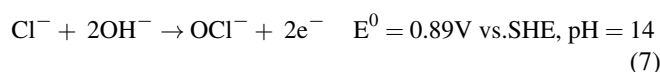
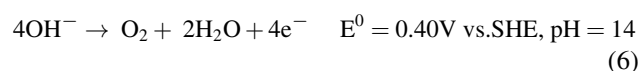
Anode competition is another challenge, because there are more anions and cations in seawater, they will compete with the water splitting reaction. Standard mean chemical composition of seawater species with the corresponding redox reaction

and electrochemical standard potential ( $E_0$ ) at different pH is shown in the table 1 [22, 24]. Due to the low concentration of some ions, their competing reactions are usually ignored, such as  $\text{Br}^-$  and  $\text{F}^-$ . The table 1 only lists ions with an average concentration greater than  $0.05 \text{ mol kg}^{-1}$  ( $\text{H}_2\text{O}$ ) in seawater [23]. As shown in the table 1, the higher concentration of  $\text{Cl}^-$  in the seawater (about  $0.5 \text{ mol kg}^{-1}$ ) will compete with the oxygen evolution reaction (OER) reaction and inhibit the oxygen precipitation at the anode. Figure 1 shows the Pourbaix diagram model of the artificial seawater system at room temperature. It can be seen that the reaction at the anode during the electrolytic seawater reaction is as follows equations (4)–(7) [23]:

In acidic conditions:



In alkaline conditions:

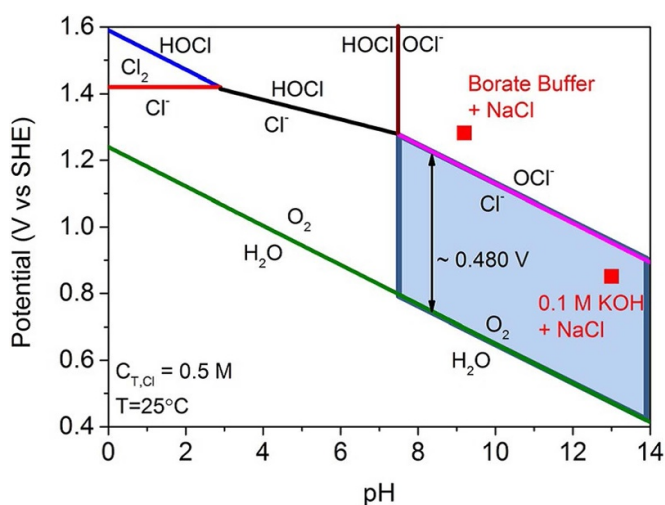


More importantly, the OER reaction suffers from high energy barrier and slow kinetics of seawater electrolysis as a four-electron transfer process. It is well known that the equilibrium potential of the OER is 1.23 V (equation (4)) in acidic solutions (0.40 V in alkaline conditions (equation (6))), which is preferred over that of the chlorine evolution reaction 1.36 V (equation (5)) in acidic solutions (0.89 V in alkaline conditions (equation (7))). However, chlorine evolution reaction is two-electrons reaction with fast kinetics, so when the potential difference is not large, affected by factors such as pH, temperature, it is very easy to compete with OER under acidic conditions. Therefore, the optimal design and preparation of high-selectivity and high-efficiency anti-corrosion OER electrocatalysts are the focus of seawater electrolysis research.

Traditional noble metal-based materials, such as Pt, Ir, Ru electrocatalysts, whose exposed active sites are highly selective for OER in seawater splitting, are therefore considered highly active electrocatalysts [25–27]. But because of their scarcity and high cost, so it is extremely difficult to be promoted on a large scale. Therefore, it is of great importance to develop electrocatalysts with low cost, abundance in raw materials, and large output [28]. Non-noble metal electrocatalysts have been widely used in OER research in recent years, including transition metal borides/carbides/nitrides/phosphides/oxides/chalcogenides/hydroxide, perovskites, and carbon materials [29]. Among them, transition metal alloys and their composites have attracted widespread interest due to their ability to balance price, performance, and durability. Many reviews have discussed them in detail [30, 31]. Layered double hydroxide and carbon materials, due to the advantages

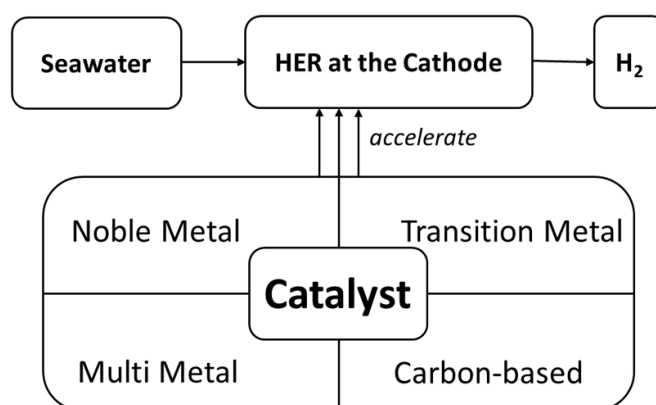
**Table 1.** Standard average chemical composition of typical seawater species with corresponding redox reactions and electrochemical standard potential  $E_0$  at different pH.

species	Conc. (mol/kg(H <sub>2</sub> O))	Redox Reaction at pH = 0	$E_0$ (V <sub>SHE</sub> )	Redox Reaction at pH = 14	$E_0$ (V <sub>SHE</sub> )
H <sub>2</sub> O	—	$2\text{H}_2\text{O} \rightleftharpoons \text{O}_2 + 4\text{H}^+ + 4\text{e}^-$	1.229	$\text{H}_2 + 2\text{OH}^- \rightleftharpoons 2\text{H}_2\text{O} + 2\text{e}^-$	-0.828
H <sup>+</sup>	—	$\text{H}_2 \rightleftharpoons 2\text{H}^+ + 2\text{e}^-$	0.0	—	—
OH <sup>-</sup>	—	—	—	$4\text{OH}^- \rightleftharpoons \text{O}_2 + 2\text{H}_2\text{O} + 4\text{e}^-$	0.401
Cl <sup>-</sup>	0.56576	$2\text{Cl}^- \rightleftharpoons \text{Cl}_2(\text{g}) + 2\text{e}^-$	1.358	$\text{Cl}^- + 4\text{OH}^- \rightleftharpoons \text{ClO}_2^- + 2\text{H}_2\text{O} + 4\text{e}^-$	0.76
		$\text{Cl}^- + 4\text{H}_2\text{O} \rightleftharpoons \text{ClO}_4^- + 8\text{H}^+ + 8\text{e}^-$	1.389	$\text{Cl}^- + 2\text{OH}^- \rightleftharpoons \text{ClO}^- + \text{H}_2\text{O} + 2\text{e}^-$	0.89
		$\text{Cl}^- + 3\text{H}_2\text{O} \rightleftharpoons \text{ClO}_3^- + 6\text{H}^+ + 6\text{e}^-$	1.451	$2\text{Cl}^- \rightleftharpoons \text{Cl}_2(\text{g}) + 2\text{e}^-$	1.358
		$\text{Cl}^- + \text{H}_2\text{O} \rightleftharpoons \text{HClO} + \text{H}^+ + 2\text{e}^-$	1.482	—	—
		$\text{Cl}^- + 2\text{H}_2\text{O} \rightleftharpoons \text{HClO}_2 + 3\text{H}^+ + 4\text{e}^-$	1.570	—	—
Na <sup>+</sup>	0.48616	$\text{Na} \rightleftharpoons \text{Na}^+ + \text{e}^-$	-2.71	$\text{Na} \rightleftharpoons \text{Na}^+ + \text{e}^-$	-2.71
Mg <sup>+</sup>	0.05475	$\text{Mg} \rightleftharpoons \text{Mg}^{2+} + 2\text{e}^-$	-2.372	$\text{Mg} \rightleftharpoons \text{Mg}^{2+} + 2\text{e}^-$	-2.372

**Figure 1.** Pourbaix diagram for artificial seawater model. [23] John Wiley & Sons. [© 2016 WILEY-VCH Verlag GmbH & Co. KGaA, Weinheim].

of in-plane electron transfer mode, abundant active sites at edges, and high specific surface area, therefore has excellent OER performance, regarded as one of the most promising catalysts, besides, carbon material can also play a stable metal role in hydrolysis as a carrier, and increase its OER activity by modifying the defect position [32]. Graphene in carbon materials as an effective catalyst carrier has great potential due to its high stability and electronic migration rate and high tolerance for impurities of seawater [33].

The cathode problem is also a problem which cannot be ignored. Compared with the strong acid and alkali ( $\text{pH} > 12$ ) environment of electrolyzed fresh water, seawater is mainly neutral. Under such conditions, the **catalyst activity is low**. Furthermore, HER reaction occurring at the cathode leads to a dramatic pH increase near the electrode, when the value is greater than 9.5, calcium and magnesium ions in seawater will combine with hydroxides to form insoluble substances, such as calcium oxide and magnesium hydroxide. These impurities are easily attached to the catalyst surface, thus hindering the direct contact between the electrolyte and the catalyst active sites, thus severely **reducing the catalyst life** in seawater electrolysis. Most reported HER catalysts to decay by more than

**Figure 2.** Types of catalysts for HER from electrolyzed seawater.

50% within 24 h in seawater electrolysis [34]. These issues require researchers to develop 'new corrosion-resistant electrolysis seawater catalysts'.

In order to solve the key bottleneck of large-scale production and utilization of hydrogen production from seawater, poor catalyst activity and stability catalysts for hydrogen evolution reaction (HER) in seawater, researchers have carried out some research on this issue [22]. A series of HER catalysts synthesized and prepared, some of which show excellent catalytic activity and can be stable for a period of time in seawater. According to the type and quantity of elements, they can be classified into the following categories (figure 2): (i) Noble metal catalyst; (ii) Transition metal catalyst; (iii) Multi metal catalyst; (iv) Carbon based catalyst.

The review listed these types of catalysts, and selected some of the data to compare their catalyst activities, as shown in figure 3, noble metals show higher electron transport capacity and lower overpotential, such as Pt, Pd, Ir, Ru, etc [35–38]. However high cost, easily to be poisoned, inactivated by complex chemical, and biological environment in seawater has always plagued its performance. Compared with noble metal catalysts, transition metal catalysts such as molybdenum based, cobalt based and nickel based are widely studied due to the existence and morphological characteristics of 3d orbital electrons, they exhibit catalytic activity similar to noble metals [36, 39–44], so they are suitable as substitutes.

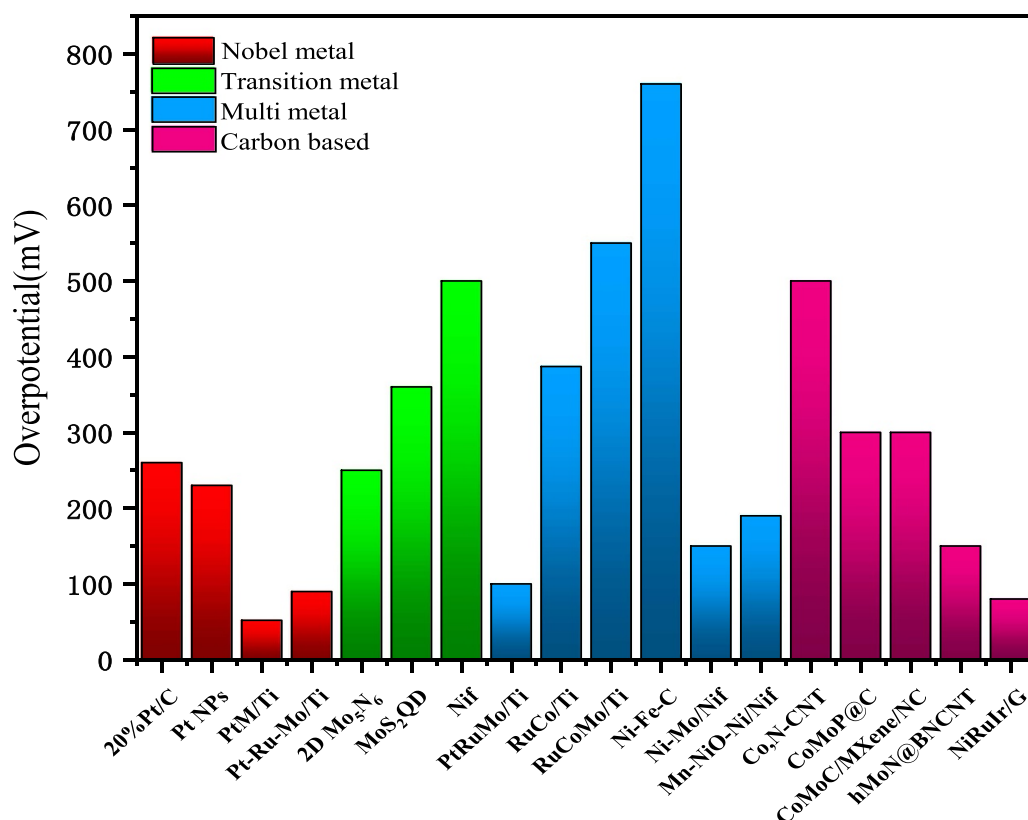


**Figure 3.** HER activity of different types of catalysts in seawater.

And it has been reported that Co based and Ni based catalysts usually cooperate with other metals, while Mo based catalysts catalyze alone. For multi metal catalyst, it is found that the rearrangement of electron cloud occurs when binary metal or multi-element metal forms alloy, resulting in surface induced potential, reducing the overpotential of catalytic reactions and reducing the activation energy required for catalytic reactions [45–47]. This is manifested as bifunctional or multifunctional synergistic catalytic effect and further improve its performance. Although metal catalysts have good performance, they have disadvantages such as high cost, low selectivity, poor durability, and poor sensitivity to gases [48]. Carbon-based catalysts can overcome many of the disadvantages of metal catalysts. It has good electrical conductivity, large specific surface area and stable physical and chemical properties, so it has been widely used in the energy field. On the other hand, for catalyst stability studies, as shown in table 2, metal catalysts based on carbon materials protect the catalyst from corrosion, agglomeration and poisoning in seawater, therefore they have better stability.

Graphene is a kind of a two-dimensional carbon-based material. A single layer of carbon atoms is closely arranged and connected by sp<sup>2</sup> hybrid orbitals to form a two-dimensional crystal. The carbon atoms are regularly arranged in the honeycomb-shaped six-membered ring lattice structure unit. In practice, graphene has a variety of defects, such as five membered rings, seven membered ring, holes, cracks, impurity atoms and so on. These defects will lead to the change of intrinsic properties of graphene (figure 4) [53]. Due to the

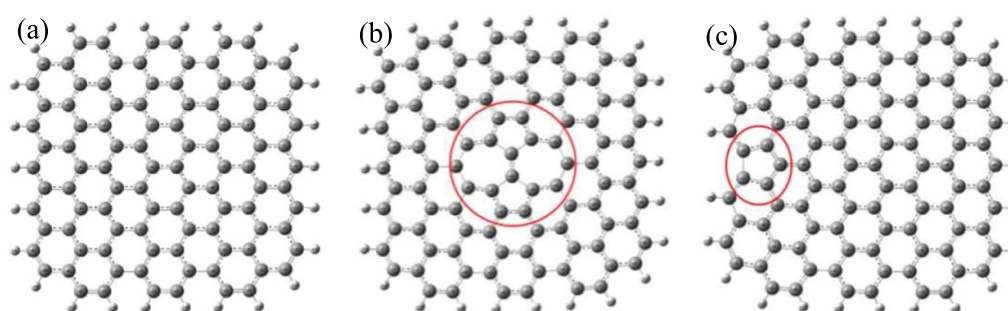
unique structural characteristics of graphene, graphene as a catalyst carrier exists in the seawater environment and has the following advantages (figure 5), it has **higher conductivity, specific surface area and better pore structure** [54, 55]. These advantages also make it one of the most widely studied and best catalyst supports [56–65]. In addition, when graphene is used as a support to compound with active material, the active material grows parallel along the direction of the graphene sheet. The active material is evenly distributed on the graphene surface, which can provide **more active sites for reaction**. Graphene can also improve the **structure and composition stability of the electrode**, and protect the metal nanoparticles from the influence of the seawater environment [56–65]. And when HER reaction occurs graphene can protect the catalyst, preventing impurities from depositing on the surface of the catalyst due to increased pH [66–69]. This review will focus on the types and properties of graphene catalysts, and propose methods for their optimal regulation and preparation methods commonly used in experiments. Finally, some potential future development directions for graphene-based catalysts are proposed.

### 3. Graphene-based catalyst and performance regulation approach

According to the combination of graphene and catalyst, graphene can be used in the following three types of catalysts for hydrogen production from seawater electrolysis: (i) Graphene as substrate, coupled with the catalyst to support the

**Table 2.** Compare the HER performance in real seawater between different types of catalysts reported in literature.

Type	Catalyst	Tafel slope (mV dec <sup>-1</sup> )	Overpotential (V)	Stability
Noble metal catalyst	20%Pt/C [49]	—	~0.26(vs RHE)	The current density drops sharply after 8 h
	Pt NPs [39]	45.8	~0.23(vs RHE)	No significant drop in current density within 10 h
	PtM/Ti [50]	—	~0.052(vs RHE)	The overpotential remains at 0.60 within 10 h
	Pt-Ru-Mo/Ti [39]	99.8	~0.092(vs RHE)	The overpotential remains at 0.80 within 180 h
Transition metal catalyst	2D Mo <sub>5</sub> N <sub>6</sub> [41]	66.0	~0.25(vs RHE)	The overpotential remains at 0.30 within 100 h
	MoS <sub>2</sub> QDareogel [42]	—	~0.36(vs RHE)	The potential remains stable after 150 cycles
	Nif [43]	165(PB ph7)	~0.5(vs RHE)	—
Multi metal catalyst	PtRuMo/Ti [39]	44	~0.1(vs RHE)	The current density drops by 15% after 172 h
	RuCo/Ti [36]	107	0.387(vs RHE)	The current density drops by 30% after 12 h
	RuCoMo/Ti [36]	140	0.550(vs RHE)	No significant drop in current density within 12 h
	Ni-Fe-C [51]	—	~0.76(vs Hg/HgO)	—
	Ni-Mo/Nif [52]	105	~0.15 (vs Ag/AgCl)	—
Carbon based catalyst	Mn-NiO-Ni/Nif [43]	121	~0.185 (vs RHE)	No significant drop in current density within 14 h
	Co,N-CNT [32]	~159(PB ph7)	~0.5(vs RHE)	No significant drop in current density within 10 h
	CoMoP@C [40]	~140 (PBph7)	~0.3(vs RHE)	No significant drop in current density within 10 h
	Co <sub>x</sub> Mo <sub>2-x</sub> C/MXene/NC [46]	—	~0.3	No significant drop in current density within 200 h
	hMoN@BNCNT [37]	~128	~0.15	No significant drop in current density within 16 h
NiRuIr/G [35]	48	~0.08	The current density drops by 10% after 200 h	

**Figure 4.** (a) Atomic model diagram of the complete structure of graphene. (b) Atomic model diagram of graphene with seven-membered ring defects. (c) Atomic model diagram of graphene with five-membered ring defects. Reproduced from [53] with permission from the Royal Society of Chemistry.

catalyst on its surface; (ii) Graphene as coating, covering the surface of metal nanoparticles to form a stable core-shell structure; (iii) Graphene as composite layer, used as a conductive medium to compound with a conductive substrate and surface catalyst (figure 6).

### 3.1. Graphene-based catalyst

Graphene as a substrate combined with a catalyst to catalyze water electrolysis is familiar. As mentioned above, graphene with high electrical conductivity, specific surface area and



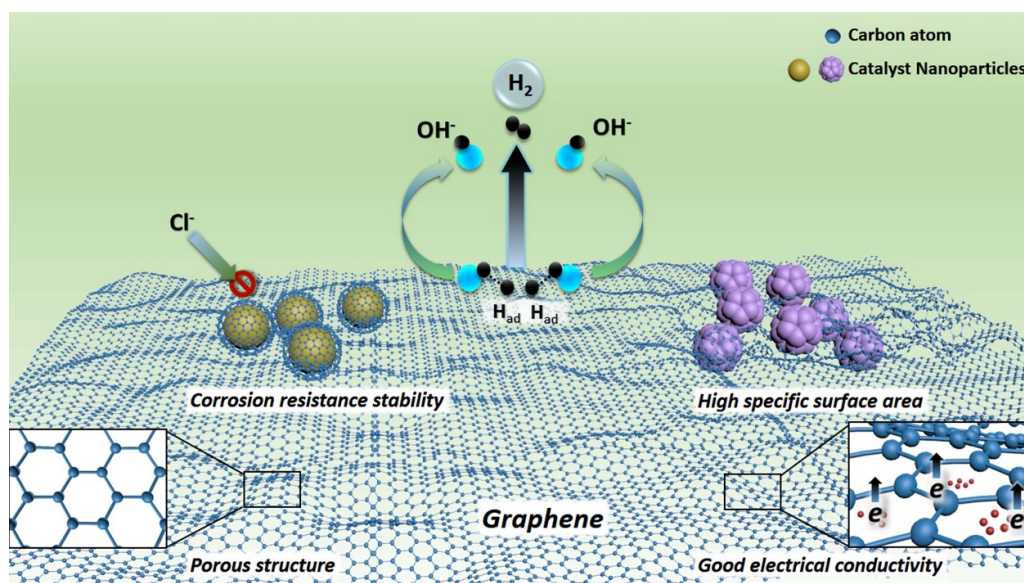


**Figure 5.** Characteristics of graphene as a catalyst for hydrogen evolution in electrolysis of seawater.

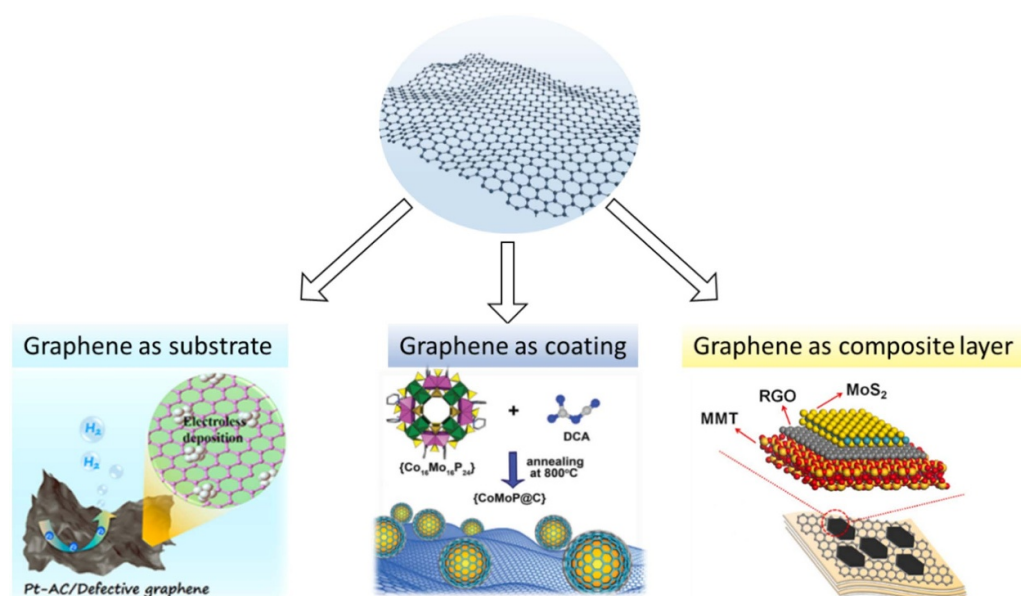


**Figure 6.** The type of graphene in regulating catalytic performance. Reprinted with permission from [70]. Copyright (2020) American Chemical Society. Reproduced from [40] with permission from the Royal Society of Chemistry. Reprinted from [71], Copyright (2020), with permission from Elsevier.

better pore structure are highly suitable as catalyst substrate materials. It can effectively improve the activity of catalysts in seawater, specifically, it includes improving its electrical conductivity and electron transfer ability, and could effectively disperse the catalytic particles and prevent their agglomeration and deactivation.

Sarno *et al* used the hydrothermal method to synthesize graphene as a conductive substrate to support the nanostructure of Ni/Ru/Ir alloy (Ni/Ru/Ir\_G). The high negative charge state on the surface of Ir can effectively repel  $\text{Cl}^-$  and increase the stability of the catalyst. The highly conductive graphene reduces the charge transfer resistance at the catalyst/electrolyte interface and improves electrochemical conductivity.

The sample exhibits a low overpotential with 100 mV in a KOH aqueous electrolyte (figure 7(a)) and a Tafel slope of  $72 \text{ mV dec}^{-1}$ , which suggests that the electrochemical hydrogen production proceeds quickly also in this case and remarkable stability (figure 7(b)). While in the real seawater system, HER overpotential of the sample is only 80 mV, and it can maintain high catalytic stability within 200 h (figures 7(c) and (d)) [38]. The experiment shows that when graphene is used as the support substrate, the coupling effect between graphene and catalyst, the dispersion of catalyst on its surface and the surface properties are the main factors affecting the catalytic activity and stability of electrolytic seawater, and it is ideal for perfecting as catalyst in seawater.

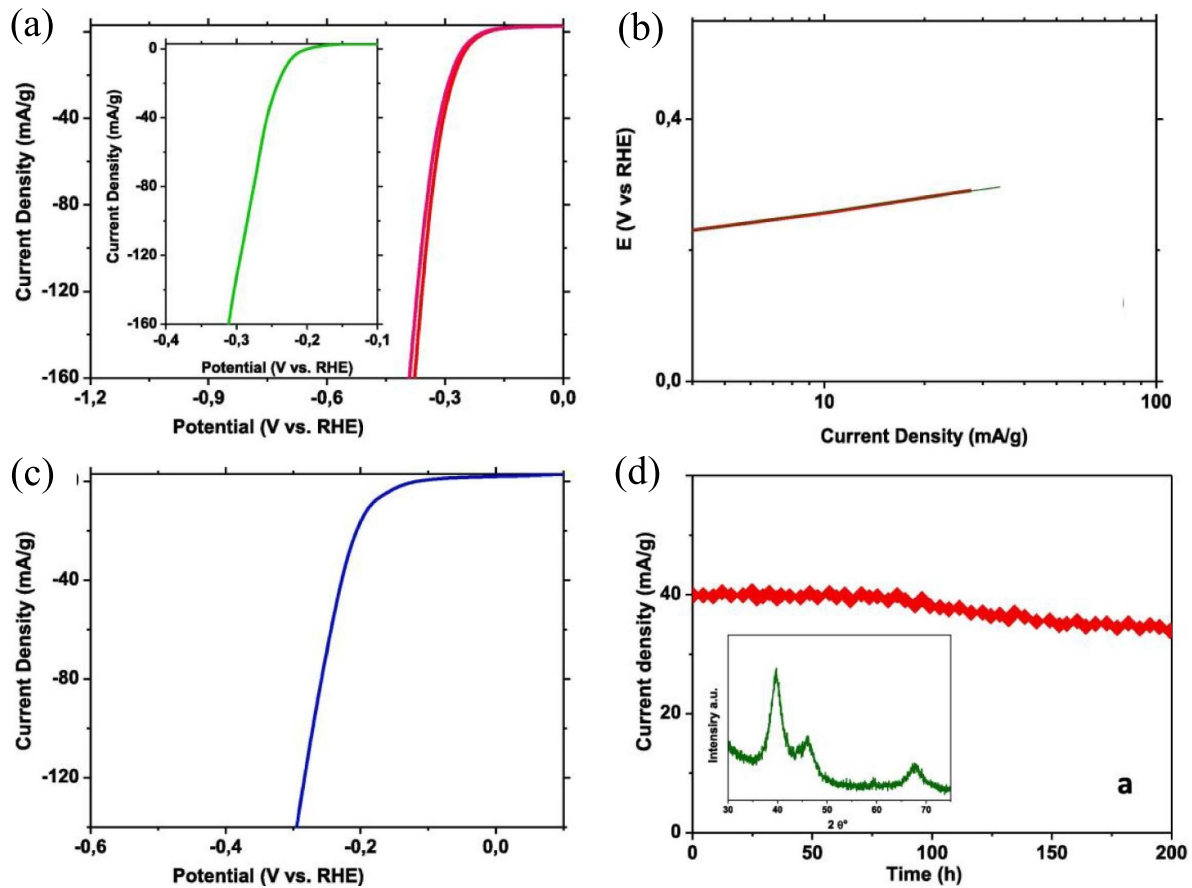


**Figure 7.** (a) Polarization curve before and after 11 000 cycles recorded at  $20 \text{ mV s}^{-1}$  in a KCl aqueous electrolyte, in the inset polarization curve recorded at  $20 \text{ mV s}^{-1}$  in a KOH aqueous electrolyte. (b) Tafel plot of NiRuIr\_G nano hybrid recorded at  $20 \text{ mV s}^{-1}$  in a KCl aqueous electrolyte. (c) Polarization curve of NiRuIr\_G nano hybrid recorded at  $20 \text{ mV s}^{-1}$  in real seawater. (d) Current-Time curve of NiRuIr\_G nano hybrid in real seawater. Reprinted from [38], Copyright (2020), with permission from Elsevier.

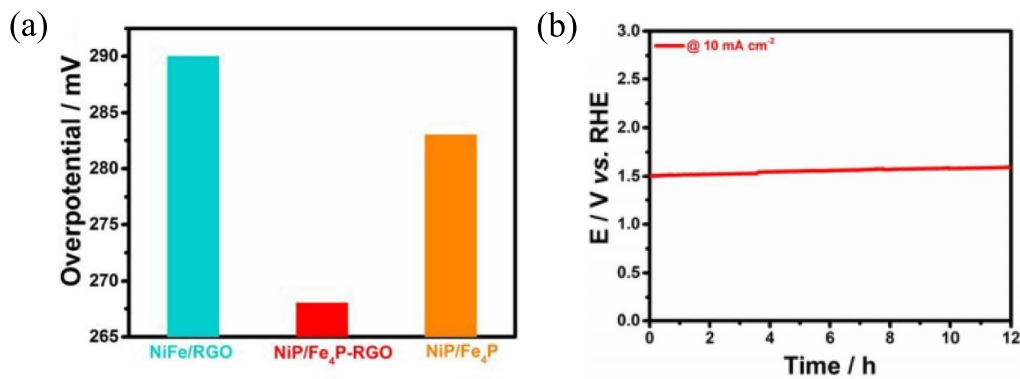


**Figure 8.** (a) The overpotential histograms of the different catalysts at  $10 \text{ mA cm}^{-2}$ . (b) CP curve of the NiP/Fe<sub>4</sub>P/RGO at a constant current density of  $10 \text{ mA cm}^{-2}$ . Reproduced from [72], with permission from Springer Nature.

Besides performing excellent performance in HER, Graphene catalysts as substrates also have the same effect in OER. Zhuang *et al* used 2D reduced graphene oxide (RGO) supported NiP/Fe<sub>4</sub>P nanosheets as OER electrocatalysts through a facile wet chemical and subsequent in situ phosphating method. The electrochemical measurements reveal that an oxidation overpotential of 268 mV with a nominal

current density of  $10 \text{ mA cm}^{-2}$ , along with outstanding long-term electrochemical stability (figure 8) [72]. It is attributed to the high specific surface area of graphene, as well as good stability.

At present, the research of graphene in seawater electrolysis mainly focuses on the catalyst substrate, but as mentioned above, graphene can also be used as coating, composite



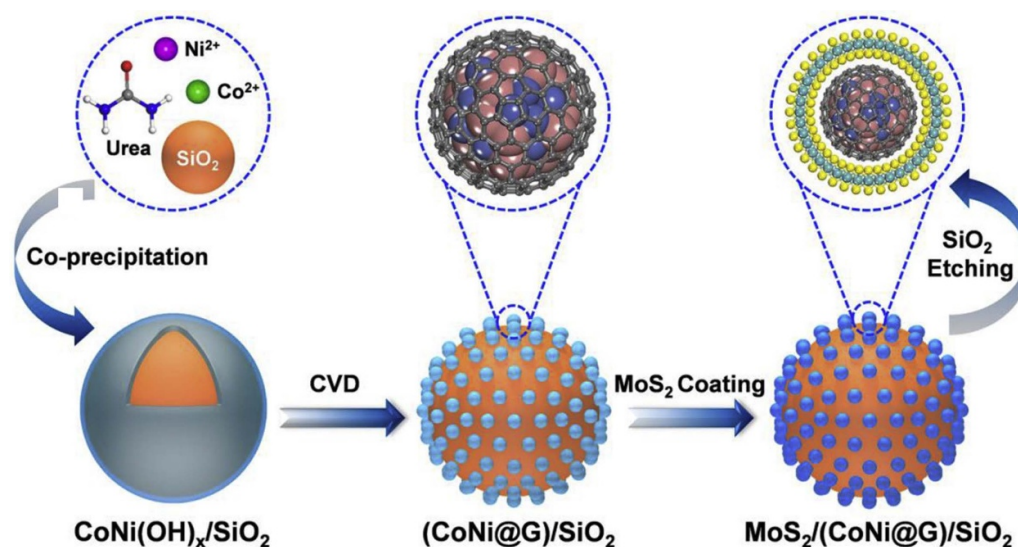


**Figure 9.** Synthetic schematic diagram of CoNi nano-alloy packaged with a double-layer  $\text{MoS}_2$ /graphene hybrid structure on  $\text{SiO}_2$ . Reprinted from [68], Copyright (2020), with permission from Elsevier.

layer, and related research has been done, such as graphene as coating, it has been reported that when graphene is used as a coating to encapsulate metal nanoparticles, it includes single-layer encapsulation and multilayer composite encapsulation. The single-layer graphene-coated CoNi nanoparticle catalyst was synthesized by Deng *et al.* The DFT theoretical calculations show that due to the difference in the work function between graphene and CoNi, part of the internal electrons in the metal core are transferred to the graphene surface, resulting in the work function of local graphene surface increases. This improves the ability of the graphene surface to activate atoms, thereby greatly enhancing HER catalytic activity [64]. Tu *et al.* prepared a CoNi nano-alloy packaged with a double-layer  $\text{MoS}_2$ /graphene hybrid structure (figure 9) [68]. Electrons in the CoNi nano-alloy pass through the graphene to reach the outermost  $\text{MoS}_2$  layer. The catalyst shows excellent HER activity and stability. In addition, the author also believes that single-layer graphene may cause the risk of low catalytic stability in harsh reaction environments, while the double-layer graphene layer can well balance catalytic activity and durability.

The core-shell structure is a special coating structure that effectively utilizes the catalyst performance and stability of graphene, and has many applications in electrolysis of water. Li *et al.* synthesized the core-shell structure of  $\text{NiSe}_2$ @nitrogen-doped graphene ( $\text{NiSe}_2$ @NG) [73] (figure 10(a)). Nickel-containing nanoparticles serve as the main catalytic core, and N-doped graphene was constructed the shell structure to increase the stability of the catalyst. The optimized special coating core-shell structure exhibits excellent electrocatalytic performance. It reveals a low onset potential of  $-163$  (or  $-171$ ) mV vs RHE, a small overpotential of  $201$  (or  $248$ ) mV vs RHE at  $10 \text{ mA cm}^{-2}$  (figures 10(b) and (c)) and particularly a low Tafel slope of  $36.1$  (or  $74.2$ )  $\text{mV dec}^{-1}$  in acid (base) (figures 10(d) and (e)).

Excellent cycling and long time stability are another advantage for hybrid mixture, which is attributed to its unique core-shell structure, apart from significantly improving the electrical conductivity and creates many active sites for enhanced electrocatalytic activity, it also ensures the chemical and structural stability of the  $\text{NiSe}_2$  core, the improves the stability of the electrocatalyst [73]. This work provides a new idea for the design and synthesis of highly performance and stable electrocatalysts.

Li *et al.* [74] first reported N-doped graphene-like carbon layers (NGCLs) coated  $\text{Ni}_3\text{S}_2$  nanowires. In terms of catalyst structure, NGCLs, as the conductive shell of the catalyst, has the function of protecting the core, especially the nitrogen-doped graphene increases the active sites of graphene, and its catalytic performance and conductivity are improved. The shell synthesized by chemical vapor deposition (CVD) method not only has more microporous structure on the surface but also provides more stable mechanical properties for the core catalyst; the core is nickel composite material  $\text{Ni}_3\text{S}_2$ , which is a transition metal chalcogenide, with high efficiency and economic characteristics, overpotentials of  $271 \text{ mV}$  and  $134 \text{ mV}$  at  $10 \text{ mA cm}^{-2}$  in  $1.0 \text{ M KOH}$  for OER and HER, respectively. Highly durable OER and HER performance demonstrated by  $40 \text{ h}$  chronopotentiometer and  $10\,000 \text{ CV}$  cycle tests.

Although the current research on the catalytic performance of the core-shell structure in seawater is mostly concentrated on non-carbon substrates [75–78]. Graphene as a two-dimensional material has stable physical and chemical properties. It has a stable carbon layer if as coating, which can effectively protect the catalyst metal from direct contact with the seawater electrolyte [66]. At the same time, using graphene as the coating layer allows the electrons of the metal core to pass through the carbon layer, and regulates the electronic structure of the carbon layer on the surface, thus promoting the catalytic reaction on the surface of the carbon layer

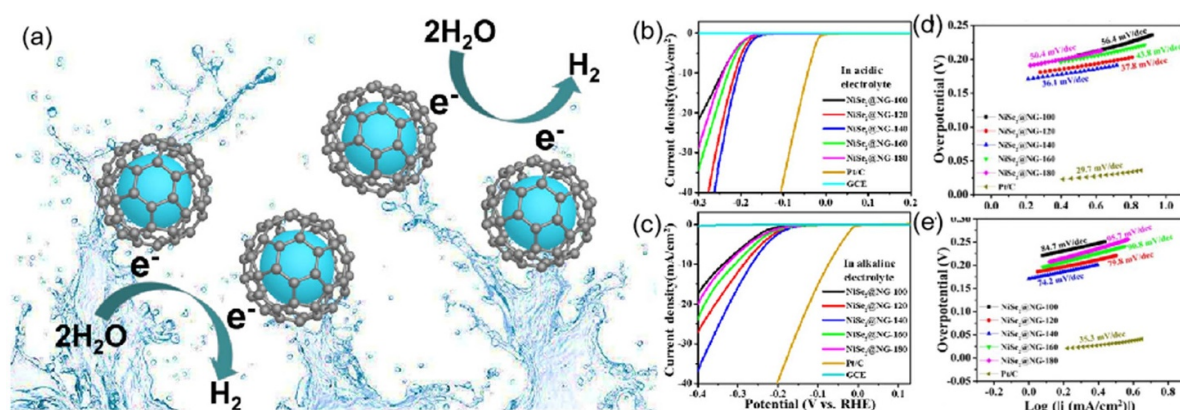


**Figure 10.** (a) Schematic diagram of the catalytic principle of the core-shell structure. (b) Electrochemical performance of the NiSe<sub>2</sub>@NGs. LSV curves in (b) acidic and (c) alkaline solutions. Corresponding Tafel plots of Pt/C catalyst and NiSe<sub>2</sub>@NGs in (d) acidic and (e) alkaline media. Reprinted with permission from [73]. Copyright (2019) American Chemical Society.

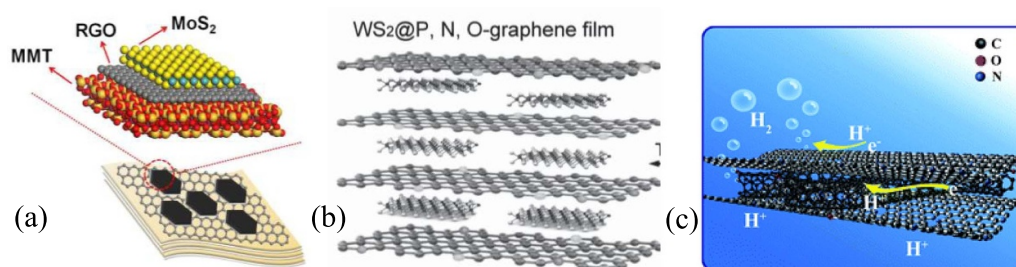


**Figure 11.** (a) Structure diagram of MoS<sub>2</sub> nanosheets on MMT modified with RGO. Reprinted from [71], Copyright (2020), with permission from Elsevier. [82] John Wiley & Sons. [© 2015 WILEY-VCH Verlag GmbH & Co. KGaA, Weinheim]. Reproduced from [83] with permission from the Royal Society of Chemistry.

[66]. We believe this will be a promising research direction, if the related core-shell structure is used in seawater catalysis.

Graphene as composite layer, Graphene can be used as a conductive substrate to directly support a catalyst and as a shell structure to encapsulate a catalyst, and it can also be used as a conductive medium to be doped into a conductive substrate or catalyst [71]. There are single-layer composite and multilayer composite in the reported results. Single-layer composite means that graphene can be used as a single-layer medium doped between the electrode and the catalyst to improve the electron transfer efficiency of the composite catalyst [78–81]. Multi-layer composite is the composite of graphene and catalyst layer by layer, so that the catalytic material can be sandwiched between the graphene sheets to form a stable graphene self-supporting 3D electrode, avoiding the electrode assembly process [82]. These designs can improve both its stability and catalyst activity.

Kang *et al* synthesized MoS<sub>2</sub> nanosheets on montmorillonite (MMT) modified with RGO by the hydrothermal method, and successfully prepared a layered ternary two-dimensional nanocomposite material (figure 11(a)), graphene is doped between the electrode and the catalyst as a single-layer conductive medium. The high conductivity of RGO and the excellent hydrophilicity of MMT can simultaneously improve the electron transfer efficiency and interface reaction efficiency of the MoS<sub>2</sub> nanocomposite. The prepared MoS<sub>2</sub>@RGO/MMT has a low Tafel slope, only about 53 mV dec<sup>-1</sup> [71]. Duan

*et al* used a vacuum filtration process to assemble 2D WS<sub>2</sub> nano-layers and P, N, and O-doped graphene sheets layer by layer into a heterostructure film to prepare a 3D catalyst electrode (figure 11(b)). The strong synergistic effect of the largest exposed active site, highly expanded surface, and continuous conductive network on the 2D nanolayer makes the structure have excellent hydrogen evolution performance [82]. A sandwich structure with one-dimensional nitrogen-doped truncated nanometers (N-TCNT) inserted between two-dimensional nitrogen-doped graphenes (NGSs) was synthesized by Li *et al* (figure 11(c)). NGSs and N-TCNTs can be connected by p-p bonds and hydrogen bonds. Its unique three-dimensional structure can provide a larger specific surface area, more electron transfer channels and sufficient reaction space, which improves its stability and HER performance [83]. The superior performance of this structure has great potential in seawater electrolysis.

Ji *et al* [28] synthesized a structure using graphene as a composite layer, stacked by graphene, MoS<sub>2</sub> and FeCoNi(OH)<sub>x</sub> (figure 12(a)). It is a typical single-layer composite which used as a single-layer medium doped between the electrode and the catalyst, so graphene also provides rapid and efficient charge transfer paths of the composite catalyst. And high specific surface area and better pore structure also ensure full exposure towards the electrolyte and easy gas release. As a result, the composite electrode can achieve an excellent OER performance with a low overpotential of 225 and 241 mV

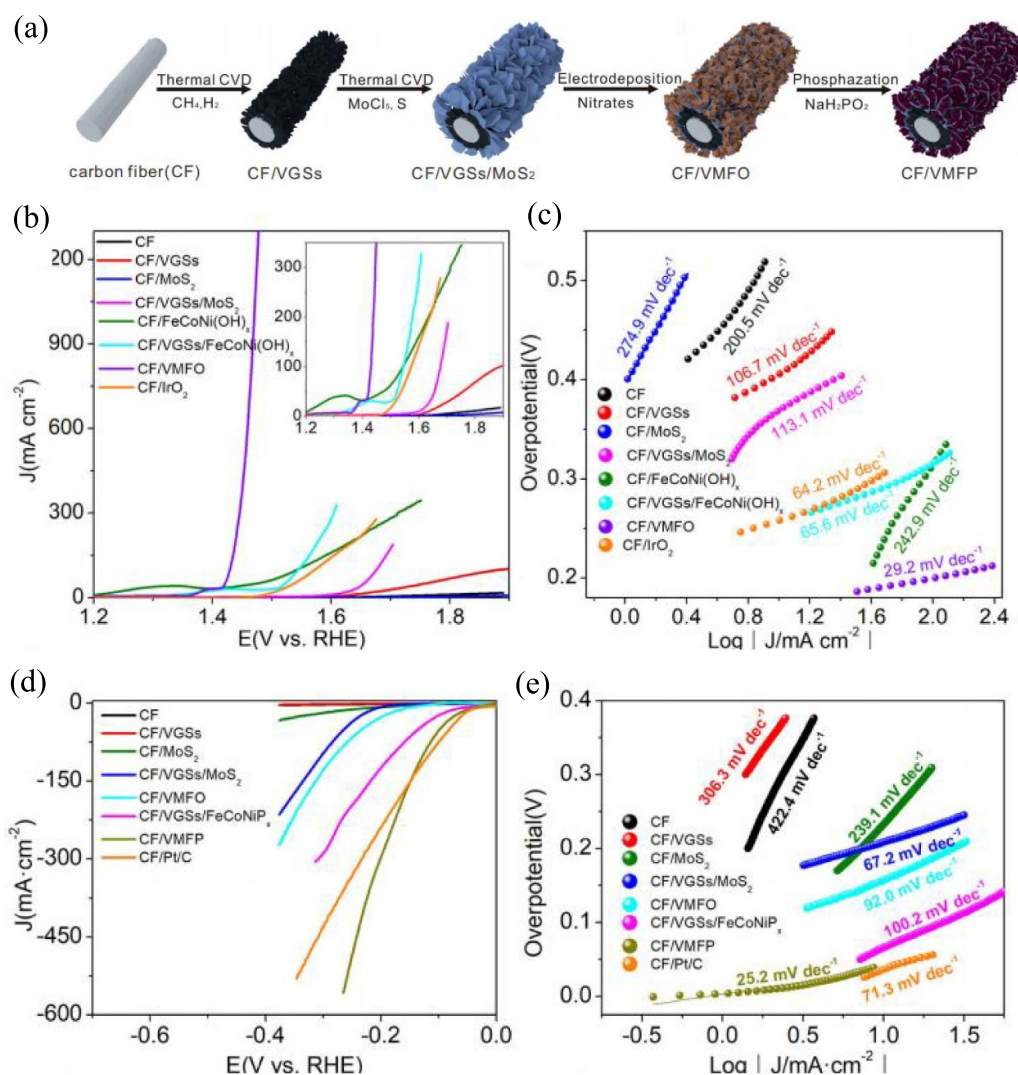


**Figure 12.** (a) Preparation procedure of CF/VMFP (b) LSV curves. (c) Tafel plots for OER performance of different samples tested in 1 M KOH. (d) LSV curves (e) Tafel plots for HER performance of different samples tested in 1 M KOH. Reproduced from [28]. CC BY 4.0.

to attain 500 and 1000 mA cm<sup>-2</sup> and 29.2 mV dec<sup>-1</sup> Tafel slope (figures 12(b) and (c)). The electrocatalytic performance of different samples for HER was also measured. As shown in figures 12(d) and (e), among the different samples including CF/Pt/C, HER performance of the CF/VMFP is the best. The overpotentials at the current densities of 10 and 100 mA cm<sup>-2</sup> are 43 and 127 mV, respectively, and the Tafel slope is 25.2 mV dec<sup>-1</sup>. In contrast, the CF/VMFO before being phosphatized exhibits an overpotential of 157 mV at 10 mA cm<sup>-2</sup> and Tafel slope of 92.0 mV dec<sup>-1</sup>.

Graphene as composite layer, can be used as a conductive substrate between the electrode and the catalyst to improve the electron transfer efficiency of the composite catalyst or can be sandwiched between the graphene sheets to form a stable graphene self-supporting 3D electrode, avoiding the electrode assembly process. Although these studies are mainly focused on the freshwater field, considering the special environment of seawater, these designs have a good protection effect on the catalyst in the face of seawater corrosion to improve both its stability and catalyst activity. So we believe that it also has

important potential in the field of electrolysis of seawater by combination of graphene.

### 3.2. Regulation approach based on graphene for catalytic performance

As mentioned above, the combination of graphene and catalyst has effectively improved the catalytic activity and stability. Furthermore, a series of regulation approaches have been conducted on graphene itself to adjust its electronic structure and the resulting catalytic performance. It should be noted that existing researches were mainly focused on electrolytic fresh water, and there was not much related research on the modified graphene used as electrolytic seawater catalysts. Owing to a certain synergistic catalytic effect of graphene to protect the matrix catalyst, it could be concluded that such strategies could also be used in the electrolytic seawater catalysts. Of course, it also needed to be further explored by combining experiments and theoretical calculations. According to the reported researches, the electronic structure of graphene was affected



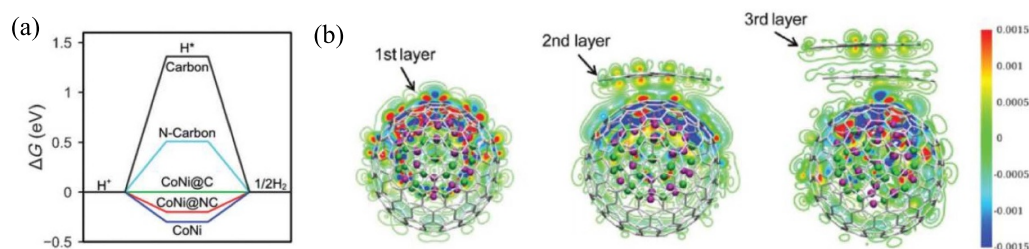


**Figure 13.** (a) Gibbs free energy ( $\Delta G$ ) profile of the HER on various catalysts. (b) Electron density distribution diagram of CoNi nanoclusters after coating one, two and three layers of graphene. [67] John Wiley & Sons. [© 2015 WILEY-VCH Verlag GmbH & Co. KGaA, Weinheim].

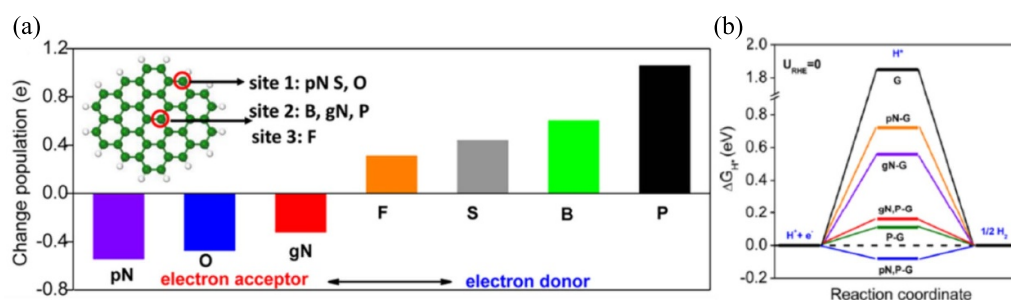


**Figure 14.** (a) NBO analysis of six different non-metallic heteroatoms in graphene. (b) Free energy of  $H^*$  adsorption after graphene doped with different atoms. Reproduced from [89]. CC BY 4.0.

by many factors, which was summarized into the following four categories including of (i) layer modification of graphene, (ii) doped atoms into graphene, (iii) coordination with different metal, and (iv) defect engineering of graphene.

**3.2.1. Layers modification of graphene.** In the synthesis of electrocatalysts, the number of graphene layers would affect the electrons transfer as well as its catalytic activity [67, 84, 85]. In Deng *et al* DFT calculations (figure 13(a)), the adsorption of  $H^*$  on the CoNi alloy was found to be too strong whereas it was too weak on the N-doped graphene shell, resulting in low HER activity in both cases. In contrast, the  $\Delta G(H^*)$  value for the graphene shells of CoNi@C can be effectively tuned by the encapsulated CoNi alloy, resulting in a high HER activity [67]. They also has developed HER catalyst coated with CoNi nanoparticles of one to three graphene layers, and it could be found that different layers of graphene exhibited significantly effect on the electron transfer between graphene and catalytic metal particles. The detailed analysis was performed by DFT (figure 13(b)), and both metal clusters and graphene layers were investigated to evaluate the effect on the electronic structure of graphene. It could be found that graphene thickness of CoNi@C catalyst played an important role on its HER performance that metal clusters generated enhanced effect on the electronic structure with relatively few layers of graphene, and thus promoting its catalytic activity [67].

**3.2.2. Doped atoms into graphene.** It has been proved by DFT theory that doping heteroatoms could effectively reduce the free energy of hydrogen adsorption ( $\Delta G_{H^*}$ ) during HER

process [86–88]. Therefore, the introduction of different heteroatoms could be an effective method to improve electronic structure as well as catalytic activity of graphene. Yao *et al* have investigated the effect of different doping heteroatom on the electronic structure of graphene by DFT [89]. Analysis of the number of natural bond orbitals (NBO) was shown in figure 14(a). It could be seen clearly that different doped atoms on the graphene surface have different number of charges. Among them, doping of N and O caused the graphene surface with negatively charged, while doping of F, S, B and P with positively charged, exhibiting different free energy of  $H^*$  adsorption when doped with different atoms into graphene (figure 14(b)). It should be noted that  $\Delta G_{H^*}$  of graphene doped with atoms was relatively lower than that of undoped state, which could be easier to promote HER process owing to improved HER activity of the catalyst [89].

**3.2.3. Coordination with different metals.** Different types of metals have different electronic structures as well as its tolerance in seawater systems. And the electronic structure of graphene would also change when combined with different types of metals. Yang *et al* have found HER activity was quite different from different metals encapsulated in the graphene shell [90]. As shown in figure 15, Co atom exhibited relatively excellent regulated capability to improve the hydrogen evolution activity of graphene compared with that of Fe atom. In addition, the catalytic performance was also affected by the size of metal atom, which determined the curvature of graphene structure that related with the distribution of electrons on the graphene surface as well as its electron transfer process, thereby affecting the rate of catalytic reaction.

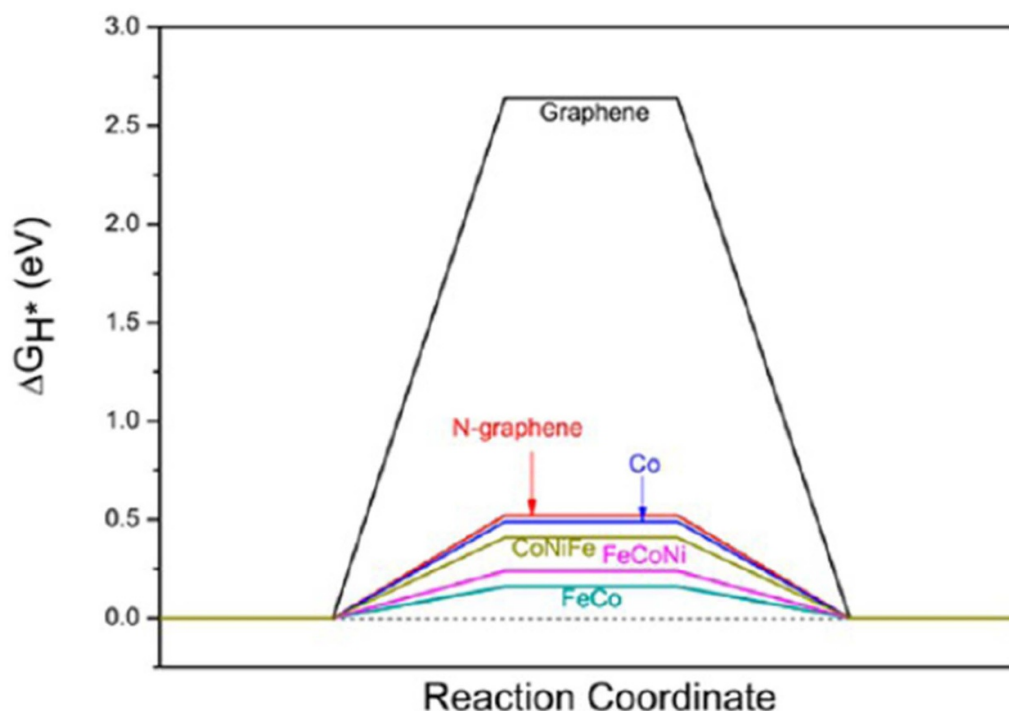


**Figure 15.** Calculated  $\Delta G_{H^*}$  diagram of Fe, Co, Ni ternary alloy and N-doped graphene. Reprinted with permission from [90]. Copyright (2016) American Chemical Society.

It is also found in currently synthesized catalysts that the smaller the size of the metal, the stronger the activity of the catalyst [66].

**3.2.4. Defect engineering of graphene.** Graphene, is of single layer two-dimensional honeycomb lattice structure, which is inherently inert to most reactions with very weak catalytic activity. In fact, there is no perfect graphene without any defects and the inherent defects of graphene also played an important role during catalytic reaction, affecting the electronic structure of graphene as well as its surface properties. Compared with perfect one, defective graphene always exhibited higher atomic binding energy with atomic utilization when supporting highly active catalysts [54, 91]. Cheng *et al* have explored the role of defective graphene (DG) in depositing and stabilizing Pt clusters through DFT calculation, where both lower work function and higher binding energy with Pt atom were found in the region of graphene with certain defects. And defect density was further investigated its effect on the hydrogen evolution performance of DG samples, and it could be found that different defect densities have significantly changed the bonding energy between graphene surface and Pt atoms. In addition, DG could also load more Pt clusters and protect them in seawater environment, which exhibited higher HER catalytic activity and stability [70].

#### 4. Preparation method of graphene-based catalyst

Graphene-based electrocatalysts can be synthesized by some effective strategies, for example, hydrothermal/solvothermal

methods, thermal treatment methods, and CVD methods. In this section, we systematically discuss the principles, methods, and advantages of these strategies. Among the various methods, the hydrothermal/solvothermal method involves the application of Teflon-lined stainless steel autoclaves, which can maintain high pressure and temperature for a long time to simultaneously achieve efficient chemical reduction of graphene oxide (GO) to graphene and to promote the nucleation and growth of metal active sites, the hydrothermal/solvothermal method is also very effective for the synthesis of graphene-based nanocatalysts with different morphologies. Heat treatment will effectively increase the degree of graphitization of graphene and induce the formation of abundant catalytic active centers. Vapor deposition is a strategy that can precisely control deposition.

##### 4.1. Hydrothermal method

Hydrothermal method is a relatively simple synthesis process for preparing graphene-based catalysts. This process has low synthesis temperature, high product purity, and easy control of the size and morphology of catalyst particles. During the process, the metal salt was first dissolved in water or organic solution, and then was uniformly dispersed by ultrasonic and subsequently moved into the reactor at a specific temperature, and finally the desired sample was obtained. Jing *et al* have synthesized a graphene-wrapped  $Ni_3S_2$  nanostructure ( $Ni_3S_2@G$ ) on the surface of foamed nickel by hydrothermal method, where expanded graphite was dispersed in formamide, and then thiourea was added as a sulfur source, subsequently the foamed nickel was introduced into the



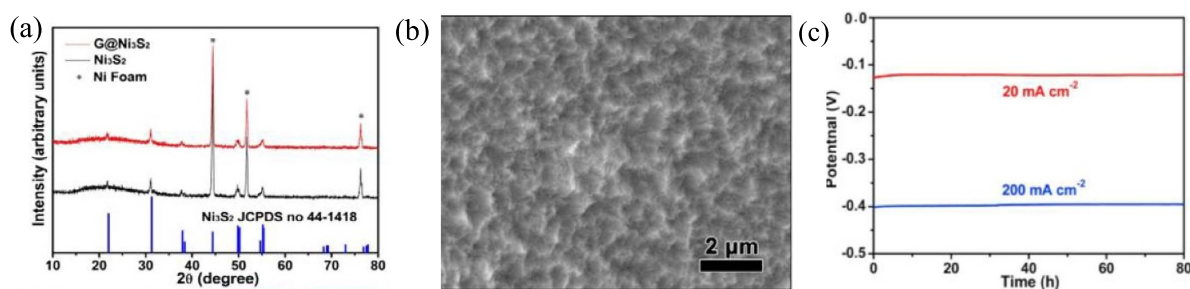


**Figure 16.** (a) XRD patterns of  $\text{Ni}_3\text{S}_2$  and  $\text{Ni}_3\text{S}_2@\text{G}$  pyramids grown on Ni foam. (b) SEM images and (c) chronopotentiometric responses of  $\text{Ni}_3\text{S}_2@\text{G}$  pyramids at the current densities of 20 and  $200 \text{ mA cm}^{-2}$  for 80 h. Reprinted from [92], Copyright (2019), with permission from Elsevier.

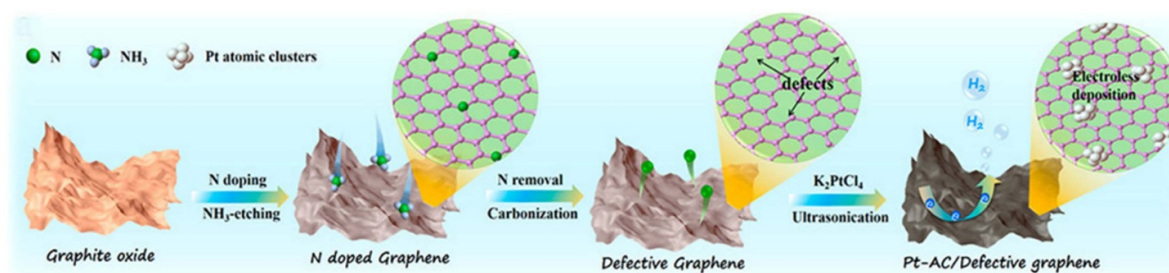


**Figure 17.** Schematic diagram of the preparation process of defective graphene-supported Pt atomic clusters. Reprinted with permission from [70]. Copyright (2020) American Chemical Society.

solution to reacted at  $180^\circ\text{C}$  for 6 h to achieve the final sample. The experimental results found that,  $\text{Ni}_3\text{S}_2$  and  $\text{Ni}_3\text{S}_2@\text{G}$  hybrid have similar XRD diffraction peaks (figure 16(a)). The three strong peaks at about  $44.4$ ,  $51.8$  and  $76.3$  originate from Ni foam substance, besides the other characteristic peaks could be indexed as the hexagonal  $\text{Ni}_3\text{S}_2$  phase with cell parameters of  $a = b = 5.7454 \text{ \AA}$ , and  $c = 7.135 \text{ \AA}$  (standard card of PDF no. 44-1418). The main peaks at  $2\theta = 21.8$ ,  $31.1$ ,  $37.7$ ,  $49.7$  and  $55.2^\circ$  are indexed as reflections from the  $(1\ 0\ 1)$ ,  $(1\ 1\ 0)$ ,  $(0\ 0\ 3)$ ,  $(1\ 1\ 3)$  and  $(1\ 2\ 2)$  crystallographic planes of hexagonal  $\text{Ni}_3\text{S}_2$ . The coat of graphene arises negligible influence on the crystal structure of  $\text{Ni}_3\text{S}_2@\text{G}$  composite [92]. More wrinkles were obtained on the sample surface after the graphene was formed, which exposed more active sites for HER process (figure 16(b)). Meanwhile, current-time curve was also measured that the graphene enhanced the stability of metal particles (figure 16(c)) [92].

#### 4.2. GO post-treatment method

GO, as a derivative of grapheme, was rich in oxygen-containing functional groups [93, 94]. GO could be obtained by oxidizing flake graphite, and then was used as a precursor to conduct high-temperature reduction in a heteroatom-containing atmosphere to finally obtain heteroatom-doped graphene. This method has the advantages of high yield and easy operation. Cheng *et al* have deposited Pt clusters on the surface of defective graphene by GO post-treatment method (figure 17). First, GO precursors were prepared by

modified Hummer's method, and then  $\text{NH}_3$  etching was applied to obtain N-doped graphene. Next, high temperature denitrication was performed to produce the defective graphene. Finally, the sample was obtained by immersing it in Pt salt solution. In this work, N doping level in graphene was controlled by adjusting  $\text{NH}_3$  etching time, and graphene samples with different defect densities were obtained by denitrication that determined HER performance of the samples [70].

#### 4.3. Chemical vapor deposition

In the practical application of graphene, the precise control of graphene layers is still a key issue. Graphene monolayers were usually prepared by CVD by exposing single crystal transition metals, such as CO, Pt, Ir, Ru, Mo and Ni, to hydrocarbon gases [95]. Chaitoglou *et al* have proposed a rapid and efficient method to synthesize a catalytic electrode of graphene growth on  $\text{Mo}_2\text{C}$  surface by CVD. In this method, Cu steam was used as a catalyst to pyrolyze  $\text{CH}_4$  to carbonize the molybdenum foil to form a  $\text{Mo}_2\text{C}$  film. By controlling the flow rate of  $\text{CH}_4$ , a vertically stacked double-layer graphene and was synthesized with  $\text{Mo}_2\text{C}$  heterostructure on the surface of molybdenum foil to obtain a graphene/ $\text{Mo}_2\text{C}$ /Mo electrode (figure 18). It has been proved that the synergy between the carbide and graphene layer promoted faster charge transfer kinetics on the catalyst surface, which could be to catalyze HER process [96].

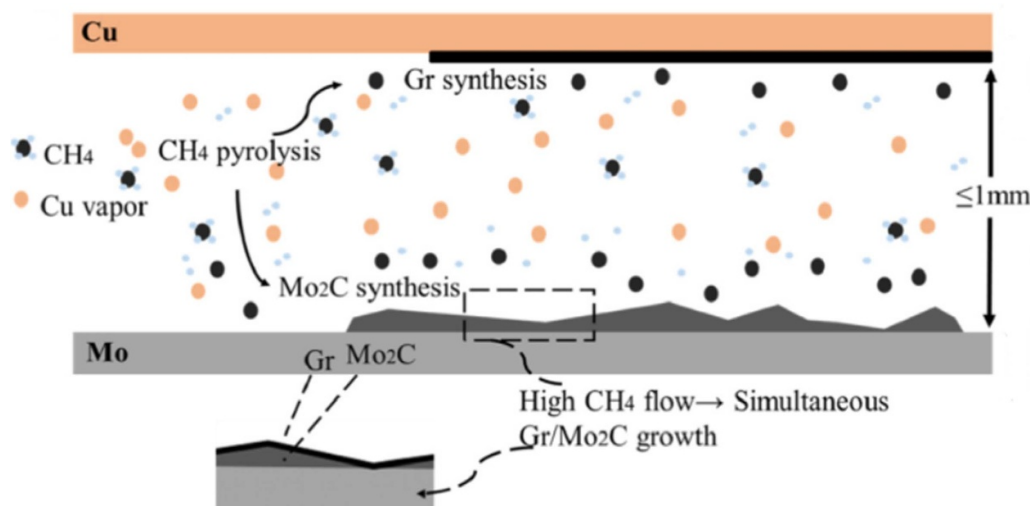


**Figure 18.** Process scheme of graphene/Mo<sub>2</sub>C/Mo electrocatalyst synthesized by copper vapor chemical vapor deposition. Reprinted from [96], Copyright (2020), with permission from Elsevier.

## 5. Future perspectives

At present, the combination of graphene and catalyst is basically divided into three categories—substrate, coating, composite layer, graphene with high electrical conductivity, specific surface area and better pore structure are very suitable as catalyst substrate materials, mainly used to improve the conductivity of catalysts. It has the characteristics of dispersing catalyst particles and improving activity, and it is also the most researched direction but only noble metals discussion in seawater electrolysis. Although the performance of catalyst is good, the cost of noble metals is too high to be widely commercialized. The studies of combination of low-cost non-precious metal catalysts and graphene need to be developed urgently. Graphene, as a coating, can form a core-shell structure to wrap on the surface of catalyst particles, effectively preventing the deactivation of catalyst performance caused by seawater soaking, so which has better catalyst activity. And highly selectivity, in addition, high conductivity and stability are another advantage of this structure, which is attributed to the properties of graphene itself. Although graphene has been used as a coating in freshwater research, so far, there has been no report on seawater research, so graphene-coated catalysts will have great potential in seawater electrolysis. Similar to the former two, graphene as a composite coating also has advantages that other structures do not have, a good and stable support structure and electron transfer efficiency. Therefore, the composite layer catalyst would have better stability and catalytic performance at high current density, with good application value under harsh seawater conditions.

The number of graphene layers and the surface doping or defect state will affect the overall performance of the catalyst. Among them, the appropriate number of graphene layers, specific atom doping and appropriate defect density are effective ways to improve HER activity and stability of the graphene synergistic catalyst splitting seawater. However, the

mechanism of the chemically modified graphene for improving the catalytic performance is still unclear. Therefore, the mechanism of the modified graphene for enhancing the catalyst activity and stability can be studied in depth. Meanwhile, when modifying graphene, commonly used synthetic preparation methods have their own limitations. Simple and convenient strategies often have insufficient ability to accurately control. In the process of combining with catalysts, a single method is usually used, and its effect is often single. Therefore, several methods can be used to improve the intrinsic catalytic performance of graphene, so as to obtain the optimal modification parameters to improve the catalytic performance of graphene. Then, in the process of combining with the catalyst, the catalytic performance of graphene and the catalytic performance of the catalyst are considered at the same time, while the catalytic performance is preserved, the synergistic effect of the two catalytic performances need to explore to, to achieve the optimal strategy of the catalyst performance.

Graphene as a two-dimensional crystal can form a heterostructure catalyst by compounding with other two-dimensional materials. Usually, this structure is composed of two or more catalyst materials, which is connected together by physical or chemical bonds [97], Most graphene composites are generally connected by Van der Waals forces [98, 99], including core-shell structure, although material stacking can lead to a significant increase in HER activity, and the use of electronic coupling when 2D materials are stacked with metal surfaces greatly reduces the contact resistance, thereby improving the electron transfer from metal surfaces to Van der Waals catalysis planar [99], but totally it is generally poor in terms of tunability, stability and corrosion resistance. More recently, heterostructures linked by covalent bonds whose vertical covalent linkages allow control of interlayer distances and their chemical properties will facilitate communication between 2D materials, while longer, sufficiently rigid and insulating molecules will have to help decouple materials; on the other hand, the additional leverage brought by the

molecular interface will improve the intrinsic properties of the material [100–102], therefore, we believe that the heterostructure composed of graphene materials will have great application potential in catalyzing seawater.

In addition, the intrinsic activity of the catalyst particles is different, and the tolerance in seawater is also different. Therefore, after different atoms are combined with graphene, its atomic structure and electronic state will change, leading to changes in the final HER performance. These catalysts have greater differences in the performance of HER in seawater. It is possible to carry out controllable preparation research on the combination of graphene and different types of catalyst particles. Researchers can prepare electrolytic electrodes in which graphene is combined with different types of catalyst particles to effectively control the surface electronic properties of graphene and metal nanoparticles. Meanwhile, it is possible to explore the type of metal with the best catalytic activity and stability after being combined with graphene.

Finally, in order to achieve overall seawater splitting, it is necessary to prepare HER and OER bifunction catalysts. Compared with the two-electron reaction process of HER, OER is a four-electron reaction process [103]. The oxygen evolution process of electrolyzed seawater on the anode is more complicated. And because there are other reactions competing with OER on the anode, not only the activity and stability of the catalyst in the seawater system should be considered when designing the OER catalyst, but also the catalytic selectivity of the catalyst. In addition, the kinetic speed of various reactions in seawater is also one of the factors to be considered. While preparing the graphene-regulated HER catalyst, its OER performance can be studied. Then, the OER catalyst is combined with the high-performance HER catalyst to explore the potential of graphene to participate in the regulation of HER/OER bifunction catalytic splitting of seawater.

## 6. Conclusion

In summary, seawater is the most abundant water resources on earth. The use of seawater electrolysis to produce hydrogen has the tremendous advantages of wide sources, low cost, and simple technology. However, it is still necessary to solve the problem of catalyst poisoning and deactivation in the seawater system. In the preparation of various HER catalysts for electrolysis of seawater, the carbon-based material graphene has the characteristics of high conductivity, large specific surface area and good stability. It can effectively protect metal nanoparticles from poisoning and deactivation in the harsh system of electrolytic seawater. The regulation of the surface structure of graphene is beneficial to improve its synergistic catalytic performance with metal catalysts. Therefore, the combination of improved graphene and metal can obtain a highly active and stable HER catalyst in seawater. This review classifies and summarizes the research progress of existing electrolysis seawater catalysts, and summarizes the applicable types of graphene in carbon-based materials in the catalytic electrolysis of water for hydrogen evolution. As a two-dimensional

carbon-based material, graphene has great practical application potential in synergistic catalytic electrolysis of seawater for hydrogen evolution. Based on the existing problems in the current electrolytic seawater system and HER mechanism of graphene under the existing system, a development direction for the graphene to synergistically regulate the electrolytic seawater hydrogen evolution catalyst is proposed.

However, the protective mechanism of graphene on enhancing the stability of catalyst particles in the seawater reaction system is still unclear, and the regulation of the structure of graphene on catalyst activity remains to be studied. In addition, due to the high dispersibility of graphene and its own catalytic properties, there should be a clearer understanding of the intrinsic activity and interaction between the catalyst and graphene.

## Acknowledgments

We gratefully acknowledge the financial support from Yunnan Precious Metals Laboratory Science and Technology Project (Grant No. YPML-2023050274) and National Natural Science Foundation of China (Grant Nos. 52231008, 52171078).

## ORCID iD

Zhong Wu  <https://orcid.org/0000-0002-5943-065X>

## References

- [1] Oh S, Cho T, Kim M, Lim J, Eom K, Kim D, Cho E and Kwon H 2017 Fabrication of Mg–Ni–Sn alloys for fast hydrogen generation in seawater *Int. J. Hydrog. Energy* **42** 7761–9
- [2] Kuang Y *et al* 2019 Solar-driven, highly sustained splitting of seawater into hydrogen and oxygen fuels *Proc. Natl Acad. Sci. USA* **116** 6624–9
- [3] Ahmed A, Al-Amin A Q, Ambrose A F and Saidur R 2016 Hydrogen fuel and transport system: a sustainable and environmental future *Int. J. Hydrog. Energy* **41** 1369–80
- [4] Choi P 2004 A simple model for solid polymer electrolyte (SPE) water electrolysis *Solid State Ion.* **175** 535–9
- [5] Trasatti S 1999 Water electrolysis: who first? *J. Electroanal. Chem.* **476** 90–91
- [6] Abdalla A M, Hossain S, Nisfindy O B, Azad A T, Dawood M and Azad A K 2018 Hydrogen production, storage, transportation and key challenges with applications: a review *Energy Convers. Manage.* **165** 602–27
- [7] Cortright R, Davda R and Dumesic J 2002 Hydrogen from catalytic reforming of biomass-derived hydrocarbons in liquid water *Nature* **418** 964–7
- [8] Wang B, Li Y and Ren N 2013 Biohydrogen from molasses with ethanol-type fermentation: effect of hydraulic retention time *Int. J. Hydrog. Energy* **38** 4361–7
- [9] Wen-Hui Y, Xiao-Chen L I U and Li L I 2013 Improving photocatalytic performance for hydrogen generation over co-doped ZnIn<sub>2</sub>S<sub>4</sub> under visible light *Acta Phys. - Chim. Sin.* **29** 151–6
- [10] Licht S *et al* 2001 Over 18% solar energy conversion to generation of hydrogen fuel; theory and experiment for efficient solar water splitting *Int. J. Hydrog. Energy* **26** 653–9



- [11] Luo Y, Zhang Z, Chhowalla M and Liu B 2022 Recent advances in design of electrocatalysts for high-current-density water splitting *Adv. Mater.* **34** 2108133
- [12] Esquiús J R and Lifeng L 2023 High entropy materials as emerging electrocatalysts for hydrogen production through low-temperature water electrolysis *Mater. Futures* **2** 022102
- [13] Yuan L, Weidong L, Han W and Siyu L 2021 Carbon dots enhance ruthenium nanoparticles for efficient hydrogen production in alkaline *Acta Phys.-Chim. Sin.* **37** 169–80
- [14] Chae S-Y, Yadav J B, Kim K-J and Joo O-S 2011 Durability study of electrospray deposited Pt film electrode for hydrogen production in PV assisted water electrolysis system *Int. J. Hydrog. Energy* **36** 3347–53
- [15] Juodkazytė J, Šebeka B, Savickaja I, Petrulevičienė M, Butkutė S, Jasulaitienė V, Selskis A and Ramanauskas R 2019 Electrolytic splitting of saline water: durable nickel oxide anode for selective oxygen evolution *Int. J. Hydrog. Energy* **44** 5929–39
- [16] Peñate B and García-Rodríguez L 2012 Current trends and future prospects in the design of seawater reverse osmosis desalination technology *Desalination* **284** 1–8
- [17] Schallenberg-Rodríguez J, Veza J M and Blanco-Marigorta A 2014 Energy efficiency and desalination in the Canary Islands *Renew. Sustain. Energy Rev.* **40** 741–8
- [18] Gao L, Yoshikawa S, Iseri Y, Fujimori S and Kanae S 2017 An economic assessment of the global potential for seawater desalination to 2050 *Water* **9** 763
- [19] Jia X, Klemeš J, Varbanov P and Wan Alwi S 2019 Analyzing the energy consumption, GHG emission, and cost of seawater desalination in China *Energies* **12** 463
- [20] Wittholz M K, O'Neill B K, Colby C B and Lewis D 2008 Estimating the cost of desalination plants using a cost database *Desalination* **229** 10–20
- [21] Xiang X and Liu X 2022 Research on the economic and environmental impacts of China's seawater desalination industry with different technologies in the macroeconomic system *Desalination* **533** 115734
- [22] Dresch S, Dionigi F, Klingenhof M and Strasser P 2019 Direct electrolytic splitting of seawater: opportunities and challenges *ACS Energy Lett.* **4** 933–42
- [23] Dionigi F, Reier T, Pawolek Z, Glied M and Strasser P 2016 Design criteria, operating conditions, and nickel-iron hydroxide catalyst materials for selective seawater electrolysis *ChemSusChem* **9** 962–72
- [24] Zhou G, Guo Z, Shan Y, Wu S, Zhang J, Yan K, Liu L, Chu P K and Wu X 2019 High-efficiency hydrogen evolution from seawater using hetero-structured T/Td phase ReS<sub>2</sub> nanosheets with cationic vacancies *Nano Energy* **55** 42–48
- [25] Lim T, Jung G Y, Kim J H, Park S O, Park J, Kim Y-T, Kang S J, Jeong H Y, Kwak S K and Joo S H 2020 Atomically dispersed Pt-N<sub>4</sub> sites as efficient and selective electrocatalysts for the chlorine evolution reaction *Nat. Commun.* **11** 412
- [26] Goryachev A, Etzi Coller Pascuzzi M, Carlà F, Weber T, Over H, Hensen E J M and Hofmann J P 2020 Electrochemical stability of RuO<sub>2</sub>(110)/Ru(0001) model electrodes in the oxygen and chlorine evolution reactions *Electrochim. Acta* **336** 135713
- [27] Ko J S, Johnson J K, Johnson P I and Xia Z 2020 Decoupling oxygen and chlorine evolution reactions in seawater using iridium-based electrocatalysts *ChemCatChem* **12** 4526–32
- [28] Ji X, Lin Y, Zeng J, Ren Z, Lin Z, Mu Y, Qiu Y and Yu J 2021 Graphene/MoS<sub>2</sub>/FeCoNi(OH)<sub>x</sub> and Graphene/MoS<sub>2</sub>/FeCoNiP<sub>x</sub> multilayer-stacked vertical nanosheets on carbon fibers for highly efficient overall water splitting *Nat. Commun.* **12** 1380
- [29] Jiang S, Liu Y, Qiu H, Su C and Shao Z 2022 High selectivity electrocatalysts for oxygen evolution reaction and anti-chlorine corrosion strategies in seawater splitting *Catalysts* **12** 261
- [30] Chen M, Kitiphatpiboon N, Feng C, Abudula A, Ma Y and Guan G 2023 Recent progress in transition-metal-oxide-based electrocatalysts for the oxygen evolution reaction in natural seawater splitting: a critical review *eScience* **3** 100111
- [31] Wang H, Weng C-C, Ren J-T and Yuan Z-Y 2021 An overview and recent advances in electrocatalysts for direct seawater splitting *Front. Chem. Sci. Eng.* **15** 1–19
- [32] Gao S, Li G-D, Liu Y, Chen H, Feng L-L, Wang Y, Yang M, Wang D, Wang S and Zou X 2015 Electrocatalytic H<sub>2</sub> production from seawater over Co, N-codoped nanocarbons *Nanoscale* **7** 2306–16
- [33] Sarno M, Sannino D, Leone C and Ciambelli P 2012 Evaluating the effects of operating conditions on the quantity, quality and catalyzed growth mechanisms of CNTs *J. Mol. Catal. A* **357** 26–38
- [34] Zhuang L, Li S, Li J, Wang K, Guan Z, Liang C and Xu Z 2022 Recent advances on hydrogen evolution and oxygen evolution catalysts for direct seawater splitting *Coatings* **12** 659
- [35] Zou X and Zhang Y 2015 Noble metal-free hydrogen evolution catalysts for water splitting *Chem. Soc. Rev.* **44** 5148–80
- [36] Niu X, Tang Q, He B and Yang P 2016 Robust and stable ruthenium alloy electrocatalysts for hydrogen evolution by seawater splitting *Electrochim. Acta* **208** 180–7
- [37] Shi Y-C, Feng J-J, Lin X-X, Zhang L, Yuan J, Zhang Q-L and Wang A-J 2019 One-step hydrothermal synthesis of three-dimensional nitrogen-doped reduced graphene oxide hydrogels anchored PtPd alloyed nanoparticles for ethylene glycol oxidation and hydrogen evolution reactions *Electrochim. Acta* **293** 504–13
- [38] Sarno M, Ponticorvo E and Scarpa D 2020 Active and stable graphene supporting trimetallic alloy-based electrocatalyst for hydrogen evolution by seawater splitting *Electrochem. Commun.* **111** 106647
- [39] Li H, Tang Q, He B and Yang P 2016 Robust electrocatalysts from an alloyed Pt–Ru–M (M = Cr, Fe, Co, Ni, Mo)-decorated Ti mesh for hydrogen evolution by seawater splitting *J. Mater. Chem. A* **4** 6513–20
- [40] Ma Y-Y, Wu C-X, Feng X-J, Tan H-Q, Yan L-K, Liu Y, Kang Z-H, Wang E-B and Li Y-G 2017 Highly efficient hydrogen evolution from seawater by a low-cost and stable CoMoP@C electrocatalyst superior to Pt/C *Energy Environ. Sci.* **10** 788–98
- [41] Jin H, Liu X, Vasileff A, Jiao Y, Zhao Y, Zheng Y and Qiao S-Z 2018 Single-crystal nitrogen-rich two-dimensional Mo<sub>5</sub>N<sub>6</sub> nanosheets for efficient and stable seawater splitting *ACS Nano* **12** 12761–9
- [42] Chen I P, Hsiao C H, Huang J Y, Peng Y H and Chang C Y 2019 Highly efficient hydrogen evolution from seawater by biofunctionalized exfoliated MoS<sub>2</sub> quantum dot aerogel electrocatalysts that is superior to Pt *ACS Appl. Mater. Interfaces* **11** 14159–65
- [43] Lu X, Pan J, Lovell E, Tan T H, Ng Y H and Amal R 2018 A sea-change: manganese doped nickel/nickel oxide electrocatalysts for hydrogen generation from seawater *Energy Environ. Sci.* **11** 1898–910
- [44] Zheng J 2017 Seawater splitting for high-efficiency hydrogen evolution by alloyed PtNi<sub>x</sub> electrocatalysts *Appl. Surf. Sci.* **413** 360–5
- [45] Liu T, Liu H, Wu X, Niu Y, Feng B, Li W, Hu W and Li C M 2018 Molybdenum carbide/phosphide hybrid nanoparticles embedded P, N co-doped carbon nanofibers for highly efficient hydrogen production in acidic,

- alkaline solution and seawater *Electrochim. Acta* **281** 710–6
- [46] Wu X, Zhou S, Wang Z, Liu J, Pei W, Yang P, Zhao J and Qiu J 2019 Engineering multifunctional collaborative catalytic interface enabling efficient hydrogen evolution in all pH range and seawater *Adv. Energy Mater.* **9** 1901333
- [47] Zhang Y, Li P, Yang X, Fa W and Ge S 2018 High-efficiency and stable alloyed nickel based electrodes for hydrogen evolution by seawater splitting *J. Alloys Compd.* **732** 248–56
- [48] Ganesan P, Sivanantham A and Shanmugam S 2017 Nanostructured nickel-cobalt-titanium alloy grown on titanium substrate as efficient electrocatalyst for alkaline water electrolysis *ACS Appl. Mater. Interfaces* **9** 12416–26
- [49] Miao J *et al* 2018 Polyoxometalate-derived hexagonal molybdenum nitrides (MXenes) supported by boron, nitrogen codoped carbon nanotubes for efficient electrochemical hydrogen evolution from seawater *Adv. Funct. Mater.* **29** 1805893
- [50] Zheng J 2017 Binary platinum alloy electrodes for hydrogen and oxygen evolutions by seawater splitting *Appl. Surf. Sci.* **413** 72–82
- [51] Song L J and Meng H M 2010 Effect of carbon content on Ni–Fe–C electrodes for hydrogen evolution reaction in seawater *Int. J. Hydrog. Energy* **35** 10060–6
- [52] Golgovici F *et al* 2018 Ni–Mo alloy nanostructures as cathodic materials for hydrogen evolution reaction during seawater electrolysis *Chem. Zvesti* **72** 1889–903
- [53] Zhang L, Xu Q, Niu J and Xia Z 2015 Role of lattice defects in catalytic activities of graphene clusters for fuel cells *Phys. Chem. Chem. Phys.* **17** 16733–43
- [54] Zhang L *et al* 2018 Graphene defects trap atomic Ni species for hydrogen and oxygen evolution reactions *Chem* **4** 285–97
- [55] Meyer J, Kisielowski C, Erni R, Rossell M D, Crommie M F and Zettl A 2008 Direct imaging of lattice atoms and topological defects in graphene membranes *Nano Lett.* **8** 3582–6
- [56] Yin H, Dou Y, Chen S, Zhu Z, Liu P and Zhao H 2020 2D electrocatalysts for converting earth-abundant simple molecules into value-added commodity chemicals: recent progress and perspectives *Adv. Mater.* **32** e1904870
- [57] Zhang Y, Tan Y W, Stormer H L and Kim P 2005 Experimental observation of the quantum Hall effect and Berry's phase in graphene *Nature* **438** 201–4
- [58] Novoselov K S, Geim A K, Morozov S V, Jiang D, Katsnelson M I, Grigorieva I V, Dubonos S V and Firsov A A 2005 Two-dimensional gas of massless Dirac fermions in graphene *Nature* **438** 197–200
- [59] Charlier J-C *et al* 2008 Electron and phonon properties of graphene: their relationship with carbon nanotubes *Carbon Nanotubes* vol 111, ed A Jorio, G Dresselhaus and M S Dresselhaus (springer) pp 673–709
- [60] Morozov S V, Novoselov K S, Katsnelson M I, Schedin F, Elias D C, Jaszczak J A and Geim A K 2008 Giant intrinsic carrier mobilities in graphene and its bilayer *Phys. Rev. Lett.* **100** 016602
- [61] Rao C N, Sood A K, Subrahmanyam K S and Govindaraj A 2009 Graphene: the new two-dimensional nanomaterial *Angew. Chem.* **48** 7752–77
- [62] Bong S, Kim Y-R, Kim I, Woo S, Uhm S, Lee J and Kim H 2010 Graphene supported electrocatalysts for methanol oxidation *Electrochem. Commun.* **12** 129–31
- [63] Lee S H, Kakati N, Jee S H, Maiti J and Yoon Y-S 2011 Hydrothermal synthesis of PtRu nanoparticles supported on graphene sheets for methanol oxidation in direct methanol fuel cell *Mater. Lett.* **65** 3281–4
- [64] Navalon S, Dhakshinamoorthy A, Alvaro M and Garcia H 2014 Carbocatalysis by graphene-based materials *Chem. Rev.* **114** 6179–212
- [65] Coleman J 2013 Liquid exfoliation of defect-free graphene *Acc. Chem. Res.* **46** 14–22
- [66] Deng J, Deng D and Bao X 2017 Robust catalysis on 2D materials encapsulating metals: concept, application, and perspective *Adv. Mater.* **29** 1606967
- [67] Deng J, Ren P, Deng D and Bao X 2015 Enhanced electron penetration through an ultrathin graphene layer for highly efficient catalysis of the hydrogen evolution reaction *Angew. Chem.* **54** 2100–4
- [68] Tu Y, Deng J, Ma C, Yu L, Bao X and Deng D 2020 Double-layer hybrid chainmail catalyst for high-performance hydrogen evolution *Nano Energy* **72** 104700
- [69] Fan X, Zhang G and Zhang F 2015 Multiple roles of graphene in heterogeneous catalysis *Chem. Soc. Rev.* **44** 3023–35
- [70] Cheng Q, Hu C, Wang G, Zou Z, Yang H and Dai L 2020 Carbon-defect-driven electroless deposition of Pt atomic clusters for highly efficient hydrogen evolution *J. Am. Chem. Soc.* **142** 5594–601
- [71] Peng K, Wang H, Gao H, Wan P, Ma M and Li X 2020 Emerging hierarchical ternary 2D nanocomposites constructed from montmorillonite, graphene and MoS<sub>2</sub> for enhanced electrochemical hydrogen evolution *Chem. Eng. J.* **393** 124704
- [72] Zhuang W, Li Z, Song M, Zhu W and Tian L 2022 Synergistic improvement in electron transport and active sites exposure over RGO supported NiP/Fe<sub>4</sub>P for oxygen evolution reaction *Ionics* **28** 1–8
- [73] Li W, Yu B, Hu Y, Wang X, Yang D and Chen Y 2019 Core-shell structure of NiSe<sub>2</sub> Nanoparticles@Nitrogen-doped graphene for hydrogen evolution reaction in both acidic and alkaline media *ACS Sustain. Chem. Eng.* **7** 4351–9
- [74] Li B, Li Z, Pang Q and Zhang J Z 2020 Core/shell cable-like Ni<sub>3</sub>S<sub>2</sub> nanowires/N-doped graphene-like carbon layers as composite electrocatalyst for overall electrocatalytic water splitting *Chem. Eng. J.* **401** 126045
- [75] Wu L, Yu L, McElhenny B, Xing X, Luo D, Zhang F, Bao J, Chen S and Ren Z 2021 Rational design of core-shell-structured CoP@FeOOH for efficient seawater electrolysis *Appl. Catal. B* **294** 120256
- [76] Zhang B, Xu W, Liu S, Chen X, Ma T, Wang G, Lu Z and Sun J 2021 Enhanced interface interaction in Cu<sub>2</sub>S@Ni core-shell nanorod arrays as hydrogen evolution reaction electrode for alkaline seawater electrolysis *J. Power Sources* **506** 230235
- [77] Zhang L, Lei Y, Zhou D, Xiong C, Jiang Z, Li X, Shang H, Zhao Y, Chen W and Zhang B 2021 Interfacial engineering of 3D hollow CoSe<sub>2</sub>@ultrathin MoSe<sub>2</sub> core@shell heterostructure for efficient pH-universal hydrogen evolution reaction *Nano Res.* **15** 2895–904
- [78] Xu X, Zhang Q, Yu Y, Chen W, Hu H and Li H 2016 Naturally dried graphene aerogels with superelasticity and tunable Poisson's ratio *Adv. Mater.* **28** 9223–30
- [79] Liu H, Chen D, Wang Z, Jing H and Zhang R 2017 Microwave-assisted molten-salt rapid synthesis of isotope triazine/heptazine based g-C<sub>3</sub>N<sub>4</sub> heterojunctions with highly enhanced photocatalytic hydrogen evolution performance *Appl. Catal. B* **203** 300–13
- [80] Yin L, Chen D, Cui X, Ge L, Yang J, Yu L, Zhang B, Zhang R and Shao G 2014 Normal-pressure microwave rapid synthesis of hierarchical SnO<sub>2</sub>@rGO nanostructures with superhigh surface areas as high-quality gas-sensing and electrochemical active materials *Nanoscale* **6** 13690–700



- [81] Hoque M A, Hassan F M, Higgins D, Choi J-Y, Pritzker M, Knights S, Ye S and Chen Z 2015 Multigrain platinum nanowires consisting of oriented nanoparticles anchored on sulfur-doped graphene as a highly active and durable oxygen reduction electrocatalyst *Adv. Mater.* **27** 1229–34
- [82] Duan J, Chen S, Chambers B A, Andersson G G and Qiao S Z 2015 3D WS<sub>2</sub> Nanolayers@Heteroatom-doped graphene films as hydrogen evolution catalyst electrodes *Adv. Mater.* **27** 4234–41
- [83] Li S, Yu Z, Yang Y, Liu Y, Zou H, Yang H, Jin J and Ma J 2017 Nitrogen-doped truncated carbon nanotubes inserted into nitrogen-doped graphene nanosheets with a sandwich structure: a highly efficient metal-free catalyst for the HER *J. Mater. Chem. A* **5** 6405–10
- [84] Chen H-A, Hsin C-L, Huang Y-T, Tang M L, Dhuey S, Cabrini S, Wu W-W and Leone S R 2013 Measurement of interlayer screening length of layered graphene by plasmonic nanostructure resonances *J. Phys. Chem. C* **117** 22211–7
- [85] Guinea F 2007 Charge distribution and screening in layered graphene systems *Phys. Rev. B* **75** 235433
- [86] Li M, Gu Y, Chang Y, Gu X, Tian J, Wu X and Feng L 2021 Iron doped cobalt fluoride derived from CoFe layered double hydroxide for efficient oxygen evolution reaction *Chem. Eng. J.* **425** 130686
- [87] Liu H, Liu Z, Wang F and Feng L 2020 Efficient catalysis of N doped NiS/NiS<sub>2</sub> heterogeneous structure *Chem. Eng. J.* **397** 125507
- [88] Wang Q, He R, Yang F, Tian X, Sui H and Feng L 2023 An overview of heteroatom doped cobalt phosphide for efficient electrochemical water splitting *Chem. Eng. J.* **456** 141056
- [89] Zheng Y, Jiao Y, Li L H, Xing T, Chen Y, Jaroniec M and Qiao S Z 2014 Toward design of synergistically active carbon-based catalysts for electrocatalytic hydrogen evolution *ACS Nano* **8** 5290–6
- [90] Yang Y, Lin Z, Gao S, Su J, Lun Z, Xia G, Chen J, Zhang R and Chen Q 2016 Tuning electronic structures of nonprecious ternary alloys encapsulated in graphene layers for optimizing overall water splitting activity *ACS Catal.* **7** 469–79
- [91] Najafi L, Bellani S, Oropesa-Nuñez R, Martín-García B, Prato M and Bonaccorso F 2019 Single-/few-layer graphene as long-lasting electrocatalyst for hydrogen evolution reaction *ACS Appl. Energy Mater.* **2** 5373–9
- [92] Yu J, Du Y, Li Q, Zhen L, Dravid V P, Wu J and Xu C-Y 2019 In-situ growth of graphene decorated Ni<sub>3</sub>S<sub>2</sub> pyramids on Ni foam for high-performance overall water splitting *Appl. Surf. Sci.* **465** 772–9
- [93] Chen D, Feng H and Li J 2012 Graphene oxide: preparation, functionalization, and electrochemical applications *Chem. Rev.* **112** 6027–53
- [94] Gao W (ed) 2015 The chemistry of graphene oxide *Graphene Oxide: Reduction Recipes, Spectroscopy, and Applications* (springer) pp 61–95
- [95] Reina A, Jia X, Ho J, Nezich D, Son H, Bulovic V, Dresselhaus M S and Kong J 2009 Large area, few-layer graphene films on arbitrary substrates by chemical vapor deposition *Nano Lett.* **9** 30–35
- [96] Chaitoglou S, Giannakopoulou T, Papanastasiou G, Tsoutsou D, Vavouliotis A, Trapalis C and Dimoulas A 2020 Cu vapor-assisted formation of nanostructured Mo<sub>2</sub>C electrocatalysts via direct chemical conversion of Mo surface for efficient hydrogen evolution reaction applications *Appl. Surf. Sci.* **510** 145516
- [97] Zhao G, Rui K, Dou S X and Sun W 2018 Heterostructures for electrochemical hydrogen evolution reaction: a review *Adv. Funct. Mater.* **28** 1803291
- [98] Blackstone C and Ignaszak A 2021 Van der Waals heterostructures-recent progress in electrode materials for clean energy applications *Materials* **14** 3754
- [99] Suragtkhuu S, Bat-Erdene M, Bati A S R, Shapter J G, Davaasambuu S and Batmunkh M 2020 Few-layer black phosphorus and boron-doped graphene based heteroelectrocatalyst for enhanced hydrogen evolution *J. Mater. Chem. A* **8** 20446–52
- [100] Vazquez Sulleiro M *et al* 2022 Fabrication of devices featuring covalently linked MoS<sub>2</sub>-graphene heterostructures *Nat. Chem.* **14** 695–700
- [101] Zhang J, Yan Y, Wang X, Cui Y, Zhang Z, Wang S, Xie Z, Yan P and Chen W 2023 Bridging multiscale interfaces for developing ionically conductive high-voltage iron sulfate-containing sodium-based battery positive electrodes *Nat. Commun.* **14** 3701
- [102] Li W, Guo X, Song K, Chen J, Zhang J, Tang G, Liu C, Chen W and Shen C 2023 Binder-induced ultrathin SEI for defect-passivated hard carbon enables highly reversible sodium-ion storage *Adv. Energy Mater.* **13** 2300648
- [103] Su H, Gorlin Y, Man I C, Calle-Vallejo F, Nørskov J K, Jaramillo T F and Rossmeisl J 2012 Identifying active surface phases for metal oxide electrocatalysts: a study of manganese oxide bi-functional catalysts for oxygen reduction and water oxidation catalysis *Phys. Chem. Chem. Phys.* **14** 14010–22